Defence Research and Development Canada | Recherche et développement pour la défense Canada

DEFENCE R&D DÉFENSE

Polarisation measurement with a dual beam interferometer (CATSI)

Exploratory results and preliminary phenomenological analysis

H. Lavoie
J.-M. Thériault
E. Puckrin
D. Dubé
DRDC Valcartier

Defence R&D Canada – Valcartier
External client report
DRDC Valcartier ECR 2004-372
June 2006

Canada

Polarisation measurement with a dual beam interferometer (CATSI)

Exploratory results and preliminary phenomenological analysis

H. Lavoie
J.-M. Thériault
E. Puckrin
D. Dubé
DRDC Valcartier

Defence R&D Canada - Valcartier

External Client Report
DRDC Valcartier ECR 2004-372
June 2006

Author

Hugo Lavoie

Approved by

Jean-Marc Garneau

Approved for release by

Gilles Bérubé

Chief Scientist

Abstract

This report presents preliminary results on the polarised long-wave infrared passive standoff detection and identification of surface contaminants and cumulus clouds using different polarisation configurations. The capability of the Compact ATmospheric Sounding interferometer (CATSI) for detecting chemical warfare (CW) surface contaminants is demonstrated from measurements of the CW simulant SF96 on water. Some polarimetric measurements of cumulus clouds were also performed to demonstrate the capability of polarisation measurements. The results obtained with the polarimetric dual-beam interferometer indicate that the signal-to-clutter ratio may be significantly improved in the infrared remote sensing of surface contamination and hard target signatures.

Résumé

Ce rapport présente les résultats préliminaires de détection et d'identification de contaminants de surface et le sondage de cumulus par télédétection passive polarisée dans l'infrarouge lointain. Les résultats de différentes configurations de polarisation sont présentés. Les capacités de détection de l'interféromètre compact pour le sondage atmosphérique (CATSI) sont démontrées à l'aide d'un simulant de contaminant de surface (SF96) sur l'eau. Des mesures de sondage de nuages cumulus ont également été effectuées pour démontrer les capacités des mesures polarimétriques. Les résultats obtenus avec le spectromètre à double port d'entrée polarisée semblent être très prometteurs pour augmenter significativement le rapport signal- arrière plan pour la télédétection passive de contaminants de surface.

This page intentionally left blank.

Executive summary

The inclusion of polarizers into the CATSI sensor system represents a new experimental approach to measure the differential polarization spectrum. This technique has been investigated in order to evaluate the potential of the differential method for the detection of liquid contaminants on water surfaces.

This report presents preliminary results on the polarised long-wave infrared passive standoff detection and identification of surface contaminants and cumulus clouds using different polarisation configurations. Results with different configuration of polarization are presented.

The capability of the Compact ATmospheric Sounding interferometer (CATSI) for detecting chemical warfare (CW) surface contaminants is demonstrated from measurements of the CW simulant SF96 on water. Some polarimetric measurements of cumulus clouds were also performed to demonstrate the capability of polarisation measurements.

The results obtained with the polarimetric dual-beam interferometer indicate that the signal-to-clutter ratio may be significantly improved in the infrared remote sensing of surface contamination and hard target signatures**.** This approach seems to be promising but many phenomenological effects of surface and cloud polarization need to be further investigated.

Lavoie, H., J.-M. Thériault, E. Puckrin and D. Dubé. 2006. Polarisation measurement with a dual beam interferometer (CATSI) - Exploratory results and preliminary phenomenological analysis. ECR 2004-372. DRDC Valcartier.

This page intentionally left blank.

Sommaire

L’incorporation de polariseurs au spectromètre CATSI constitue une nouvelle approche expérimentale pour mesurer le spectre différentiel de polarisation. Cette technique a été investiguée afin d’évaluer le potentiel de cette méthode à la détection de contaminants de surface liquide sur l’eau.

Ce rapport présente les résultats préliminaires de détection et d’identification de contaminants de surface et le sondage de cumulus par télédétection passive polarisée dans l’infrarouge lointain. Les résultats de différentes configurations de polarisation sont présentés.

Les capacités de détection de l’interféromètre compact pour le sondage atmosphérique (CATSI) sont démontrées à l’aide d’un simulant de contaminant de surface (SF96). Des mesures de sondage de nuages cumulus ont également été effectuées pour démontrer les capacités des mesures polarimétriques.

Les résultats obtenus avec le spectromètre à double port d’entrée polarisée semblent être très prometteurs pour augmenter significativement le rapport signal- arrière plan pour la télédétection passive de contaminants de surface. Cette technique semble prometteuse mais plusieurs effets phénoménologiques ont besoin de plus d’investigation.

Lavoie, H., J.-M. Thériault, E. Puckrin and D. Dubé. 2006. Polarisation measurement with a dual beam interferometer (CATSI) - Exploratory results and preliminary phenomenological analysis. ECR 2004-372. RDDC Valcartier.

This page intentionally left blank.

Table of contents

List of figures

Acknowledgements

The authors would like to gratefully thank Dr. Jim O. Jensen from U.S. Army SBCCOM for his support on this project.

This page intentionally left blank.

1. Introduction

Polarisation is one of the fundamental properties of light, along with intensity, frequency and coherence. The polarisation effect of infrared radiation could be very important in the case of detecting chemical contamination on surfaces. For this reason many techniques are being developed to exploit this phenomenology. Laboratory techniques such as IRRAS (InfraRed Reflection Absorption Spectroscopy) or PM-IRRAS (Polarisation Modulation – IRRAS) are well known in the literature for studying thin films on surfaces of metals or water. These techniques exploit the polarisation of light for the purpose of increasing the signal-to-clutter ratio in a measurement, in which the clutter is predominantly non-polarised radiation.

The intrinsic capability of CATSI (Compact ATmospheric Sounding Interferometer) to optically subtract the incoming radiation from two different ports facilitates the study of the polarisation effect from surfaces. The dual input port capability of CATSI provides the opportunity to split and optically subtract, in real-time, the two polarisation components (R_h and R_v) that are emitted from the surface element of a target onto a single detector, thereby mitigating the difficulty of achieving spatial registration.

In order to investigate the potential of detecting surface contaminants by exploitation of the polarisation effect, a few preliminary polarisation measurements were taken with the CATSI instrument. Two polarisers were added to the CATSI sensor; one was mounted on the first telescope and the other was mounted on the second telescope. The polarisation axis of each polariser could be oriented vertically (parallel) or horizontally (perpendicular). With this configuration each telescope passed a beam of linearly polarised radiation to each arm of the interferometer. As a result of the optical subtraction performed by the CATSI interferometer, the resulting spectrum corresponded to the difference between the spectra of the two polarised input beams. The two polarisers could be aligned in the same direction or at 90 degrees relative to each other (cross-polarised). In the case of cross-polarisation, the resulting radiance was the difference between the vertical and horizontal signals originating from the scene.

This report describes the preliminary polarisation results involving surface contamination and cumulus clouds that were obtained with the CATSI sensor. A tentative explanation is presented concerning the detection and identification of the surface contaminant, SF96, on water.

2. Detection principles and phenomenology

A passive long-wave infrared standoff sensor functions by exploiting the temperature difference (ΔT) that exists between a chemical cloud and the background scene. If the cloud is warmer than the background, then the spectrum of the chemical of interest will be sensed as an emission feature in the spectrum recorded by the sensor. Conversely, if the cloud is colder than the background, then the chemical of interest will be sensed as an absorption feature in the spectrum. This principle is illustrated in Figure 1a. When a liquid contaminant is present on a surface, ΔT is zero since the background (surface) and the contaminant are in contact. However, if the radiation from an external hot or cold source is reflected from the surface, then it is possible to observe the spectrum of the contaminant. In outdoor environments, the radiation from the cold sky provides a high surface-to-sky temperature difference that yields favourable detection possibilities. The radiative transfer associated with the detection of liquid surface contaminants is outlined below.

The radiative transfer intervening at a surface can be understood from simple physical arguments. Figure 1b shows a diagram and defines the parameters used to evaluate the radiance emanating from clean and contaminated surfaces exposed to an outdoor environment. For a clean surface having a reflectance R_0, the spectral radiance measured by the sensor contains two components, i.e. the emitted radiance from the surface, $B(1-R_0)$, and the cold sky radiance reflected by the surface, $L_{down} R_0$. The parameter, L_{down}, represents the downwelling radiance from the sky and B is the Planck radiance evaluated at the temperature (T) of the surface that is given by

$$B = \left(\frac{1.191 \times 10^{-12} \nu^3}{e^{\left(\frac{1.439\nu}{T}\right)} - 1} \right), \tag{1}$$

where ν is the wavenumber in cm^{-1}, and B is in W/cm^2 sr cm^{-1}. Adding these two radiance components, $B(1- R_0)$ and $L_{down} R_0$, yields an expression for the radiance of the clean surface that is given by

$$L_{clean} = B - R_0\left(B - L_{down}\right). \tag{2}$$

The radiance emanating from the contaminated surface (Fig. 1b) contains three components. The first component, $B\tau_{cont}$, is the surface (substrate) emission transmitted by the contaminant layer where τ_{cont} is defined as the transmittance of the layer. The second component, $L_{down}R_{cont}$, is the cold sky radiance reflected by the contaminated surface, where R_{cont} is defined as the reflectance of the contaminated surface. The last component, $(1-R_{cont} - \tau_{cont})B$, corresponds to the layer emission. It is obtained by application of the Kirchoff's law, which states that the emissivity is equal to the absorption of $(1- R_{cont} - \tau_{cont})$. Adding these three components yields for the radiance of the contaminated surface

$$L_{cont} = B - R_{cont}\left(B - L_{down}\right). \tag{3}$$

A quantity of interest to study the perturbation effects of a contaminant on a surface is the differential spectral radiance (ΔL) that is the radiance change (L_{cont} -L_{clean}) obtained by subtracting Eq. 2 from Eq. 3,

$$L_{cont} - L_{clean} \equiv \Delta L = (R_0 - R_{cont})\left(B - L_{down}\right). \tag{4}$$

Inspection of Eq. 4 reveals some simple facts concerning the sensitivity for detecting contaminants by passive spectral radiometry. First of all, the radiance change is proportional to the reflectance contrast (R_0 – R_{cont}) indicating that a highly reflecting surface, such as a metallic plate, offers more sensitivity for detection. Secondly, the radiance change is proportional to the radiative contrast between the Planck surface radiance and the downwelling sky radiance, (B – L_{down}). Since the downwelling radiance increases with the cloud cover, which in turn results in a decrease in the radiative contrast, the best detection possibilities are obtained for clear sky conditions where L_{down} reaches a minimum.

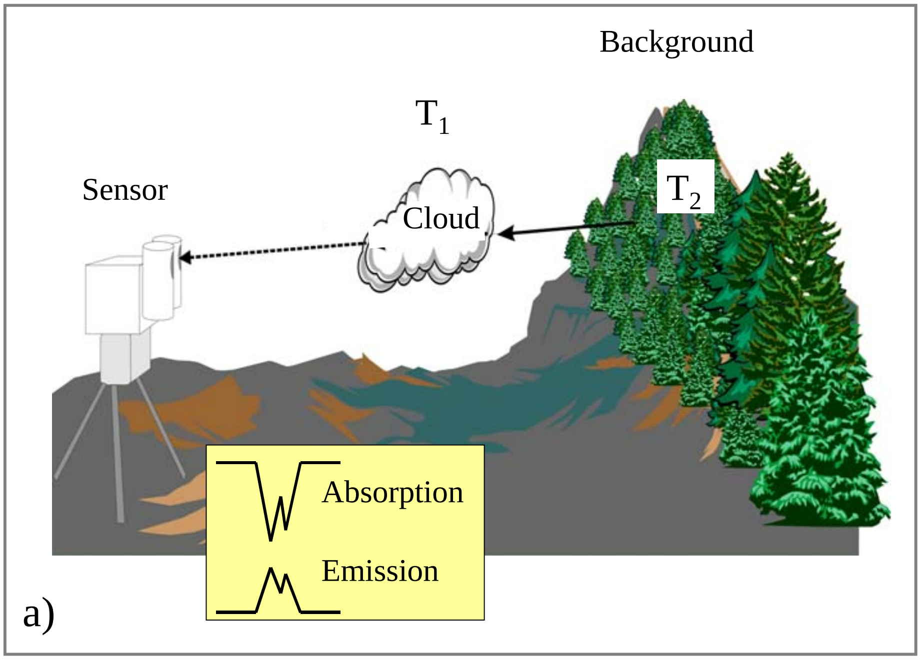

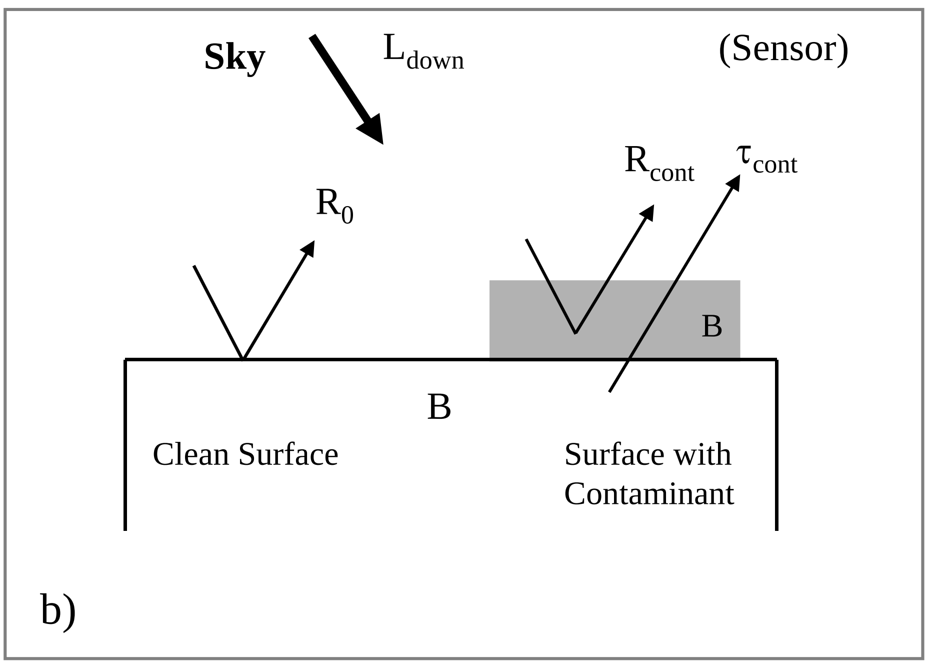

Figure 1. *(**a**) Operation of a typical long-wave infrared standoff sensor. (**b**) Diagram and parameters used to evaluate the radiance of a clean surface and a surface covered by a contaminant.*

3. Description of the CATSI sensor

The CATSI instrument is a Fourier-transform infrared (FTIR) spectrometer system that takes advantage of the differential detection capability of a symmetrical dual-beam interferometer [1,2]. CATSI was built by ABB Bomem (Quebec City) according to DRDC Valcartier contract specifications. For this system, two beams of thermal radiation originating from different scenes can be combined onto a single detector and subtracted optically in real-time.

The CATSI instrument primarily consists of two identical 10-cm diameter Newtonian telescopes optically coupled with the dual-beam interferometer. Figure 2 shows the instrument mounted on a tripod, together with a schematic diagram that summarizes the instrument's optical design. The specifications of the CATSI system are as follows: (1) scene FOV from 4 to 11 mrad, (2) spectral coverage from 7 to 13 μm, and (3) maximum spectral resolution of 1 cm^{-1}. A flat-plate mirror placed in front of each telescope can be rotated to the selected scene. The pointing capability of this scene mirror permits azimuth measurements to be made from 0 to 180 degrees. Coarse adjustments in azimuth and elevation are simply achieved by rotating the whole assembly, which is mounted on a tripod. After reflection on the scene mirror, the input beam is focused by the Newtonian telescope at the entrance of the interferometer and then reflected by an off-axis parabolic mirror to produce a collimated beam of proper diameter that impinges upon the beamsplitter.

A double-pendulum scanning mechanism controls the periodic displacement of the two corner-cube (CC) reflectors that generate the interferogram. The beamsplitter (BS) consists of a thin air gap squeezed between two ZnSe substrates having antireflection coatings on their external faces. Of the two output channels only one is used at this moment. This output module contains a parabolic and condensing mirror that focuses the radiation beam onto an MCT detector (1 mm) mounted on a microcooler. The detector is specifically optimized for the 7 – 13 μm thermal infrared band. Two CCD cameras mounted on the top of the two telescope modules are used to view the scenes under consideration.

For the measurements presented in this report, the CATSI system was operated either in differential detection mode or in direct detection mode, which was obtained by blocking one of the two input telescopes. The mode of operation was chosen according to the constraints of the observed scene.

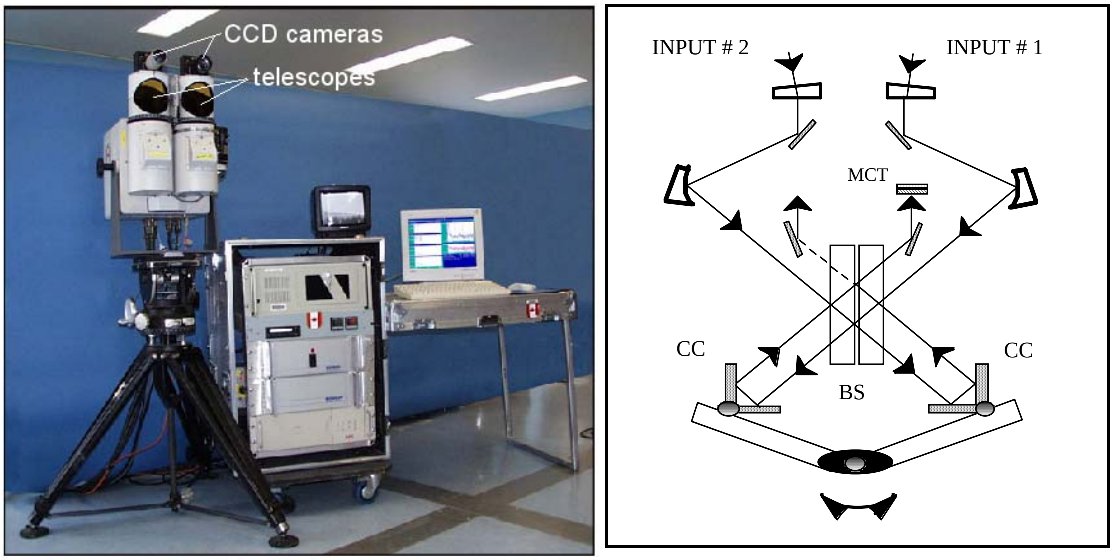

a b

Figure 2. *(**a**) Photograph of the CATSI sensor with the optical head mounted on a tripod, and (**b**) the associated optical diagram.*

4. Experimental plan and configuration

The primary objective of this report is to explore the polarisation capability of the dual input port configuration of the CATSI sensor. The preliminary polarimetric results obtained by CATSI at the SURFCON trial at DRDC Suffield in September 2002 [3] with a cross-polarised instrument configuration suggested that polarisation measurements may have a potential benefit for detecting surface contaminants. In order to further study the polarisation effect on the detectability of surface contaminants, additional measurements were performed at DRDC Valcartier with the SF96 on water.

4.1 Polarisation configuration

Figure 3 shows the polariser configurations used with CATSI for the measurement results presented in this report. A total of six different configurations were defined to obtain results on the polarisation effect of SF96 on water. Polarisers that were aligned in the same direction were used with CATSI in dual mode and direct mode. The polariser configuration is name parallel when polarisation axis is place parallel to the surface normal (configuration (a) Figure 3). The differential cross-polarisation radiance was obtained with the configurations (e) and (f) shown in Figure 3.

4.2 Surface contaminant experiments

The upper photograph in Figure 4 shows the experimental setup used to collect the spectra of SF96 on water. The pool shown in the figure was constructed of wood covered with plastic sheets. The water level was adjusted to a depth of approximately 3.8 cm for each measurement. Radiometric calibrations were first performed for clean water and these were followed immediately with measurements of the SF96 contaminant on water. Measurements were collected for at least 100 seconds to provide an indication of the radiometric stability of the studied system and the environment. The water temperature was recorded for all measurements and they showed a temperature variation of about 1 degree.

The lower photograph in Figure 4 shows the CATSI sensor looking at the water surface. The CATSI sensor was aligned at an angle of 63 degrees relative to the normal plane of the water surface.

Figure 5 shows the signature of the SF96, which is a silicon-based oil used often as a simulant for a surface contaminant [3]. The signature of SF96 was measured with a Digilab spectrometer (FTS 3000) using the diffuse reflectance FTIR (DRIFTS) technique. The spectrum was recorded at a resolution of 4 cm^{-1} using a Peltier-cooled DTGS detector and a Ge-coated KBr beamsplitter. The signature clearly shows bands at 800, 1016, 1096 and 1260 cm^{-1}.

4.3 Polarimetric measurements of clouds

The day on which polarisation measurements were collected for clouds was characterised by sky conditions that were predominantly clear with only some cumulus clouds present. Three different polariser configurations were used in this experiment, which consisted of settings (a), (d) and (e) in Figure 3.

A radiometric calibration was first performed on the clear sky and the measurements on the clouds were collected immediately afterwards. Measurements were collected for at least 100 seconds to provide an indication of the radiometric stability of the studied system and the environment.

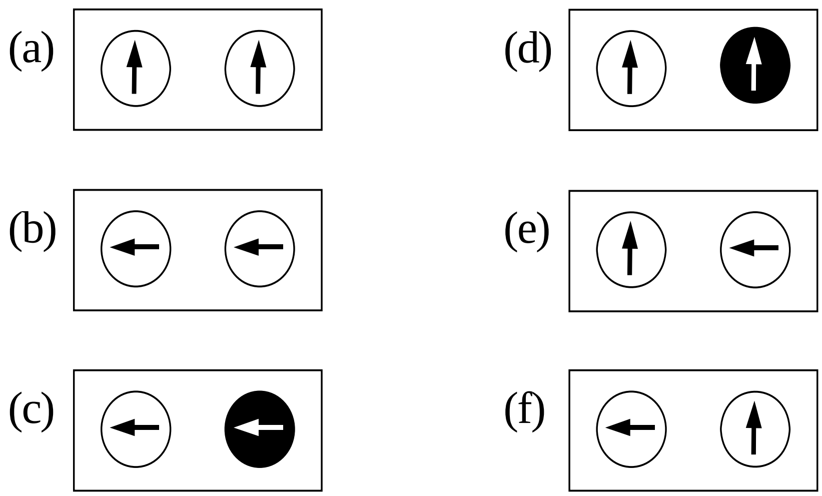

Figure 3. *Configurations of the two polarisers: (**a**) parallel polarisers (**b**) perpendicular polarisers (**c**) perpendicular polarisers with background port closed (**d**) parallel polarisers with background port closed (**e**) cross-polarised with parallel orientation in target port (**f**) cross-polarised with perpendicular orientation in target port.*

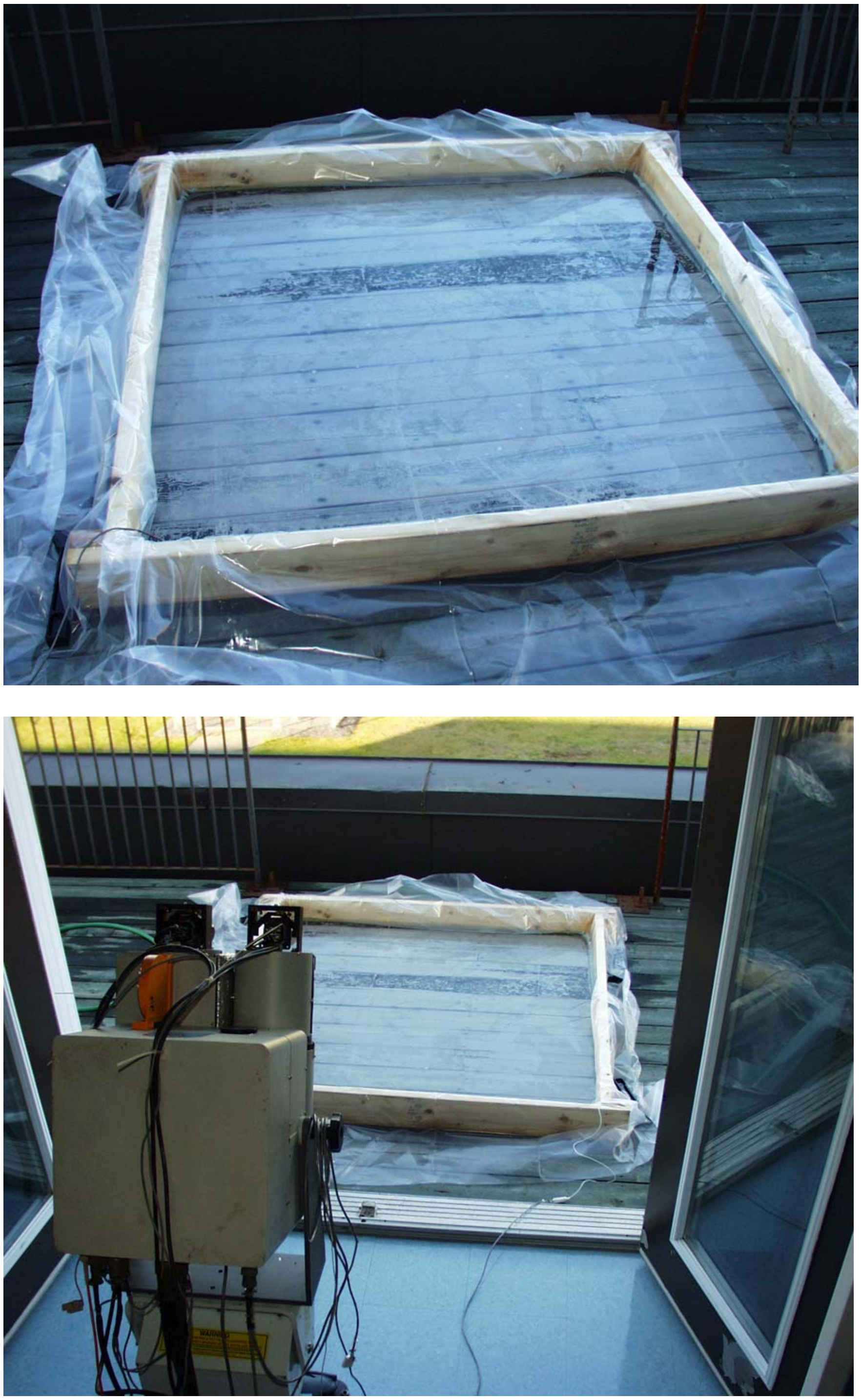

Figure 4. *Picture of the pool used for the measurements of water surface contamination (top) and the setup with the CATSI sensor (bottom).*

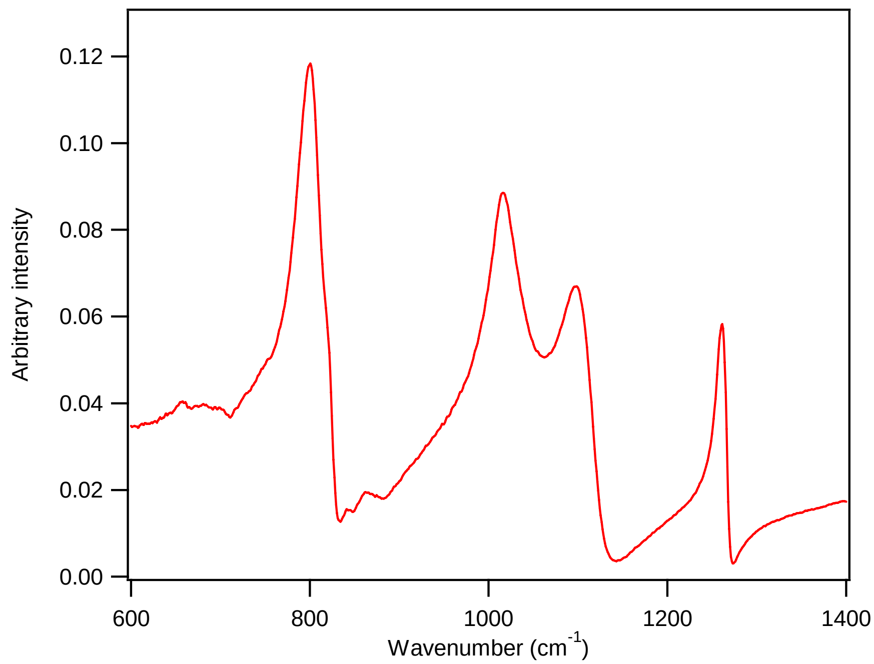

Figure 5. *Infrared signature of simulant SF96 measured with a Digilab interferometer in the same radiative region (600-1400 cm^{-1}) as CATSI sensor.*

5. Results and discussion

5.1 Polarisation measurement of water surfaces

The detection of surface contaminants on liquid surfaces such as water is a difficult problem for passive infrared standoff detectors. This is mainly due to the fact that the water absorbs a large fraction of the infrared radiation used in the passive detection process.

5.1.1 Water surface description

Figure 6 is a picture of the surface measured with the CATSI spectrometer. It can clearly be seen on the surface that the SF96 contaminant is not homogeneously distributed on the water surface. The red circles show aggregates of SF96 moving on the water surface. This effect has an impact on the CATSI measurement results, which will be discussed later in the report.

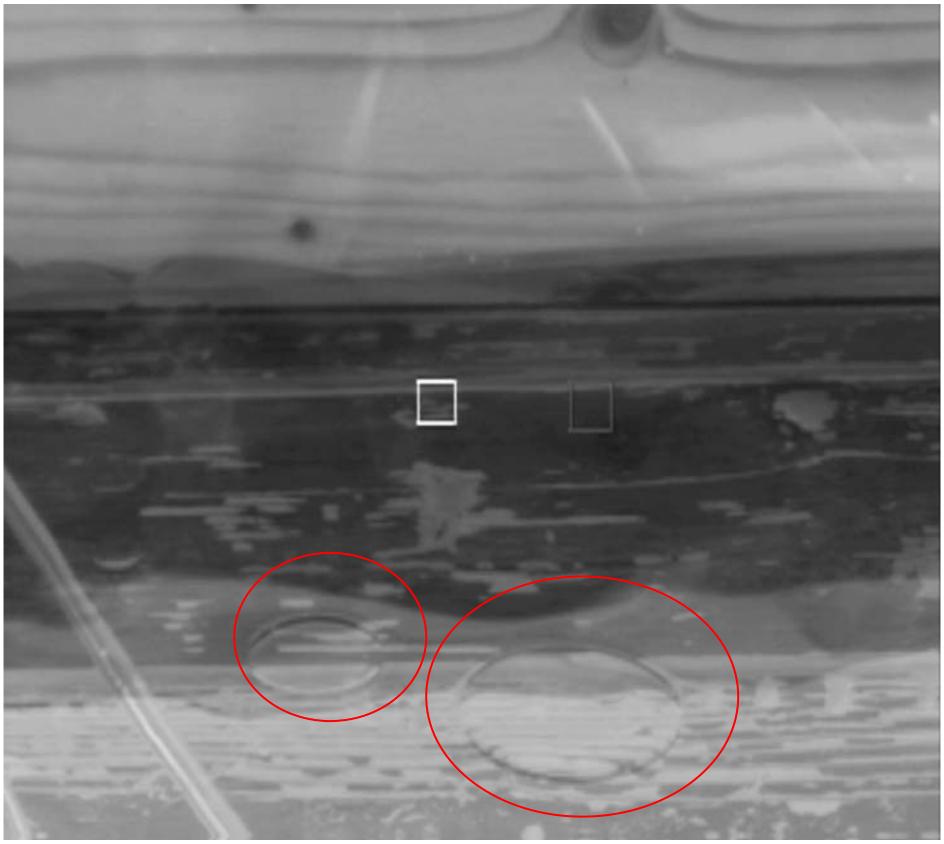

Figure 6. *Picture of the water surface after contamination. Red circles show contaminant aggregation moving on water.*

5.1.2 Polarisation measurements in direct mode

Figure 7 shows polarisation measurements taken with both polarisers aligned parallel to the surface normal of water and with the background port closed (configuration (d) in Figure 3). The upper graph in Figure 7 shows the calibrated spectrum collected for pure water. Each spectrum is composed of 20 scans collected for a period 100 s. The overlaid spectra demonstrate the radiometric stability of the measurements over time.

The lower graph of Figure 7 shows the spectra after contamination by 50 ml of SF96. The infrared signature of SF96 can be identified in these spectra. The characteristic bands are clearly distinguishable at 800, 1096 and 1260 cm^{-1}; however, the band at 1016 cm^{-1} is somewhat larger than that of the reference spectrum of SF96 shown in Figure 5. The large intensity variation can be attributed to the inhomogeneous distribution of the contaminant on the surface.

Figure 8 shows polarisation measurements performed with both polarisers aligned perpendicular to the surface normal and with the background port closed (configuration (c) in Figure 3). The upper graph in Figure 8 shows the calibrated spectra collected for pure water.

The lower graph of Figure 8 shows the spectra after contamination by 50 ml of SF96. The modification of the polarization by 90 degrees results in a large change in the spectra collected for the contaminated surface in comparison to the infrared signature of SF96 shown in Figure 5. The two major bands at 800 and 1096 cm^{-1} appear slightly shifted to higher wavenumber and the intensity of the band at 1016 cm^{-1} is much smaller than for pure SF96. There is currently no obvious explanation for this effect on the SF96 signature.

The comparison of the intensities in Figure 7 and 8 demonstrates that a polarised measurement performed with the polariser placed parallel to the surface normal of the target input port results in a significant intensity increase. This intensity of the parallel-polarised (Figure 7) spectra is approximately 10 times greater than that of the perpendicular-polarised (Figure 8) measurement. There is currently no satisfactory explanation for this significant difference in intensity.

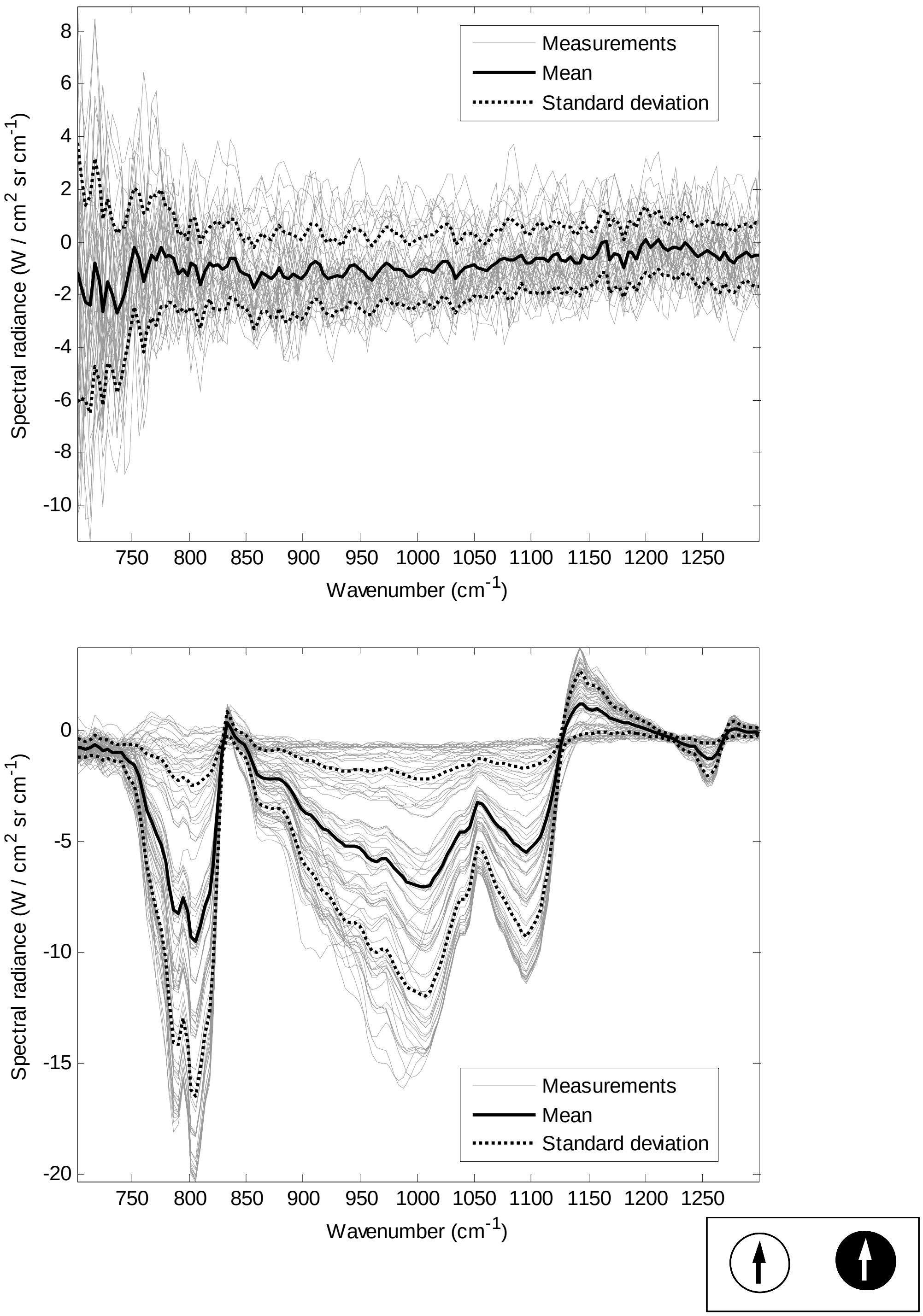

Figure 7. *Parallel-polarised measurement of SF96 on water with background port closed. Reference spectra of water (top graph) and spectra with 50 ml contamination (lower graph). The radiance values of the upper and lower graphs should be multiplied by 1×10^{-8} and 1×10^{-7}, respectively.*

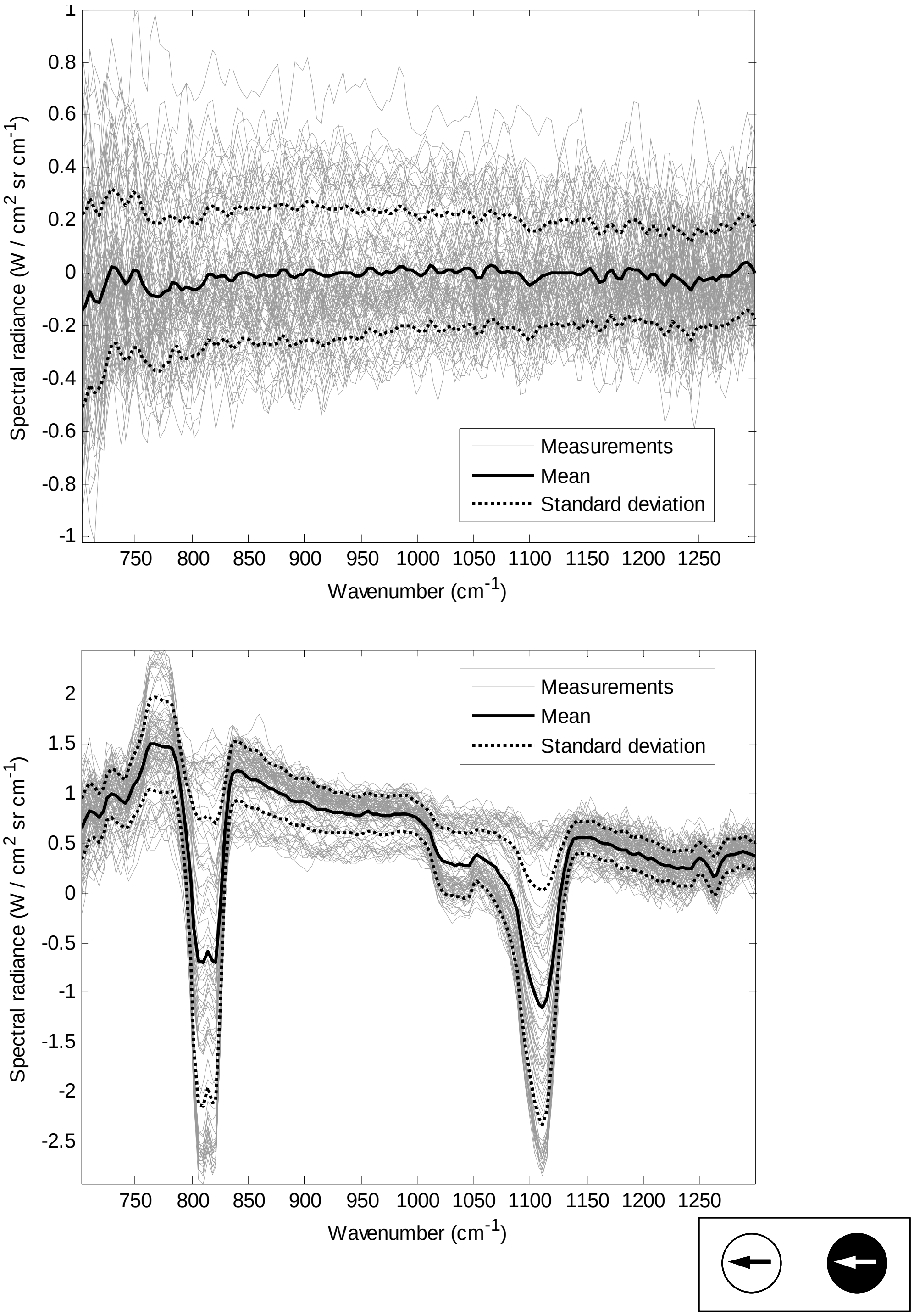

Figure 8. *Perpendicular-polarised measurement of SF96 on water with background port closed. Reference spectra of water (top graph) and spectra with 50 ml contamination (lower graph). The radiance values of the upper and lower graphs should be multiplied by 1×10^{-7}.*

5.1.3 Parallel-polarisation measurements

Figure 9 shows polarisation measurements made with both polarisers aligned parallel to the surface normal (configuration (a) in Figure 3). This experiment simulates a measurement without polarisers in the input ports. The upper graph shows the measurements for a clean water surface, and the degree of radiometric stability of the setup.

The lower graph of Figure 9 shows the spectra collected after the addition of 50 ml of SF96. The spectra show the four characteristic bands of SF96 described in Figure 5, but with a widening of the band at 1016 cm^{-1}. For these measurements it is evident that the two telescope fields of view (FOV) are not looking at the same place and for this reason the spectra collected are unstable and show both negative and positive excursions in intensity. This inversion phenomenon is directly related to the dual-port capability of CATSI in which the floating patches of SF96 move between the fields of view of the two telescopes.

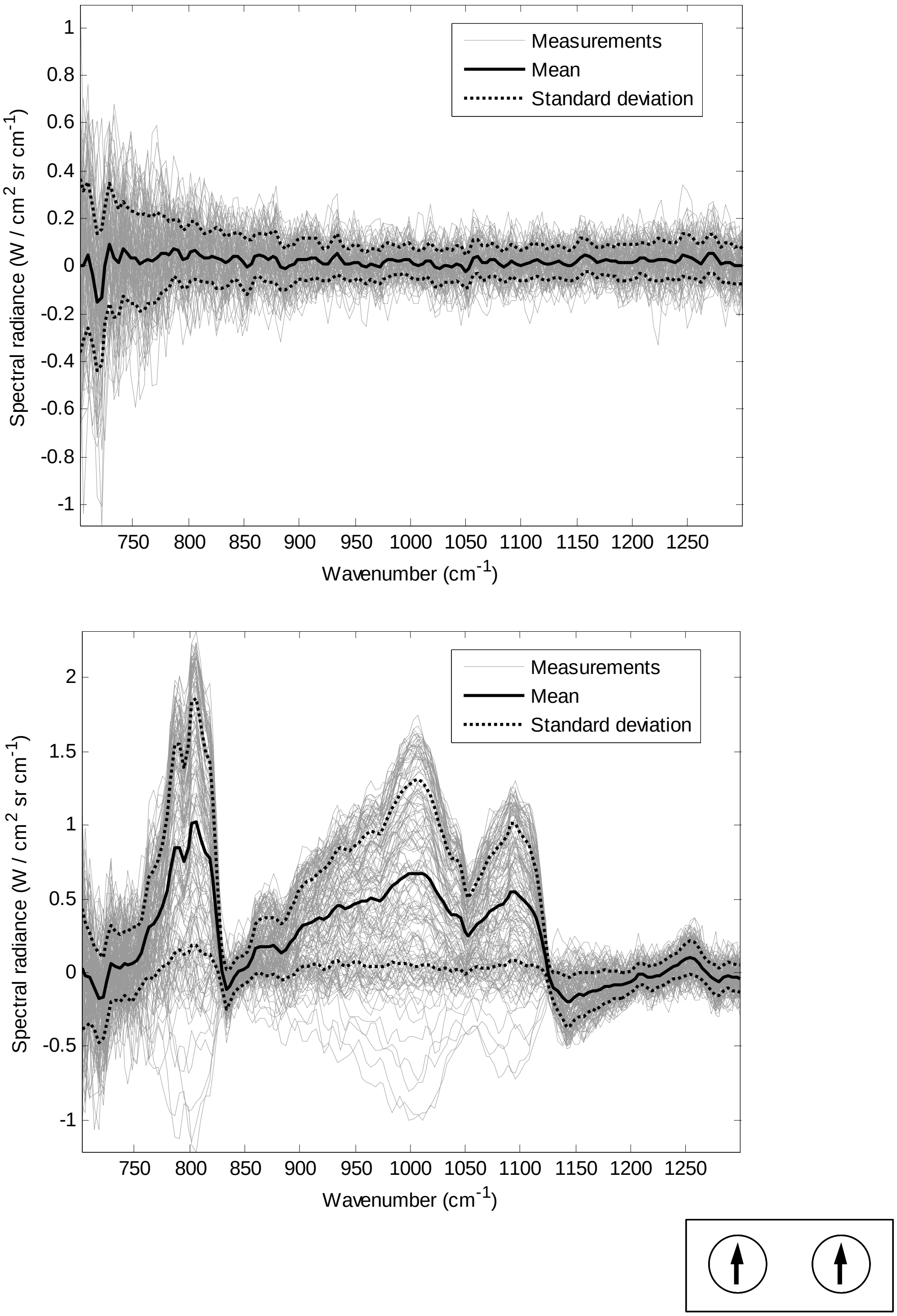

Figure 9. *Parallel-polarised measurement of SF96 on water. Reference spectra of water (top graph) and spectra with 50 ml contamination (lower graph). The radiance values of the upper and lower graphs should be multiplied by* 1×10^{-7}.

5.1.4 Cross-polarised measurements

Figure 10 shows cross-polarisation measurements performed with the polariser in the target port aligned perpendicular to the surface normal and the polariser in the background port aligned parallel with the surface normal (configuration (f) in Figure 3). The upper graph of Figure 10 shows a series of calibrated spectra of pure water. The graph demonstrates the radiometric stability of the water surface and the environment.

The middle and lower graphs of Figure 10 show the spectra collected for a SF96 contamination of 50 and 100 ml, respectively. The characteristic bands of SF96 described in Figure 5 are present in the spectra collected for both concentrations. The comparison between the spectral intensity of the two lower graphs of Figure 10 suggests that there is no significant difference in intensity upon doubling the concentration of SF96. This effect may arise due to the fact that the water surface is not yet saturated with SF96. Doubling the concentration may increase the number of SF96 patches on the water surface, but the patch density in each telescope FOV remains approximately unchanged.

Figure 11 shows cross-polarisation measurements taken with the polariser in the target port aligned parallel to the surface normal and the polariser in the background port aligned perpendicular to the surface normal (configuration (e) in Figure 3). The upper graph of Figure 11 shows the radiometric stability of the system and environment of the CATSI sensor before contamination.

The lower graph of Figure 11 shows the spectrum collected after the addition of 50 ml of SF96 contaminant. The characteristic bands of SF96 are clearly identified but the comparison with the spectra in Figure 10 shows a distinguishable negative contribution in the band at 800 cm^{-1}. This negative band cannot be identified but it could occur due to a difference in the refractive index resulting from different thicknesses of the contaminant over the water surface.

The comparison of the radiance intensities in Figure 10 and 11 demonstrates that a cross-polarised measurement made with a polariser placed parallel to the surface normal in the target input port gives a significant intensity increase. The intensity of the parallel-polarised measurement (Figure 11) is more than twice as large as the intensity for the perpendicular-polarised (Figure 10) configuration. There is currently no satisfactory explanation for this significant difference in intensity.

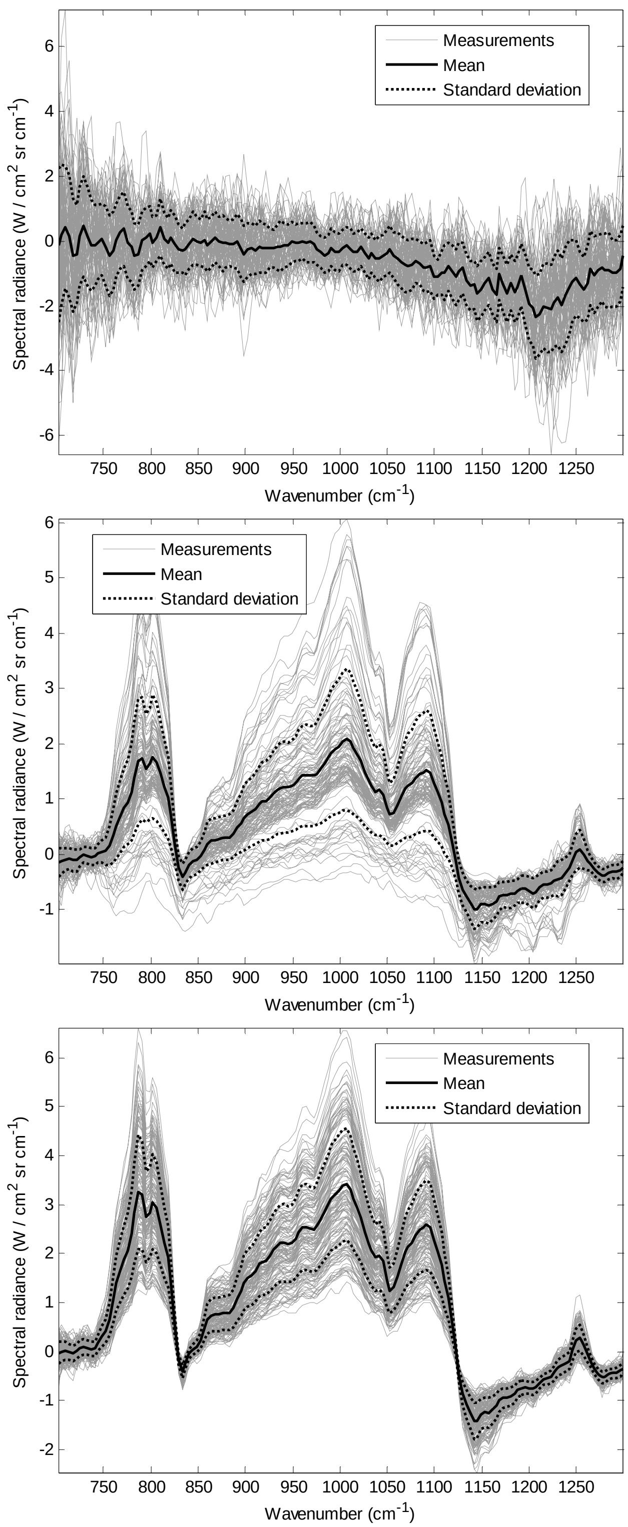

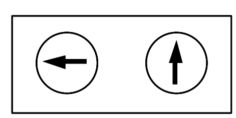

Figure 10. *Cross-polarised measurement of SF96 on water. Reference spectra of water (top graph), spectra with 50 ml contamination (middle graph), and spectra with 100 ml contamination (lower graph). The radiance values of the upper, middle and lower graphs should be multiplied by 1×10^{-8}, 1×10^{-7} and 1×10^{-7}, respectively.*

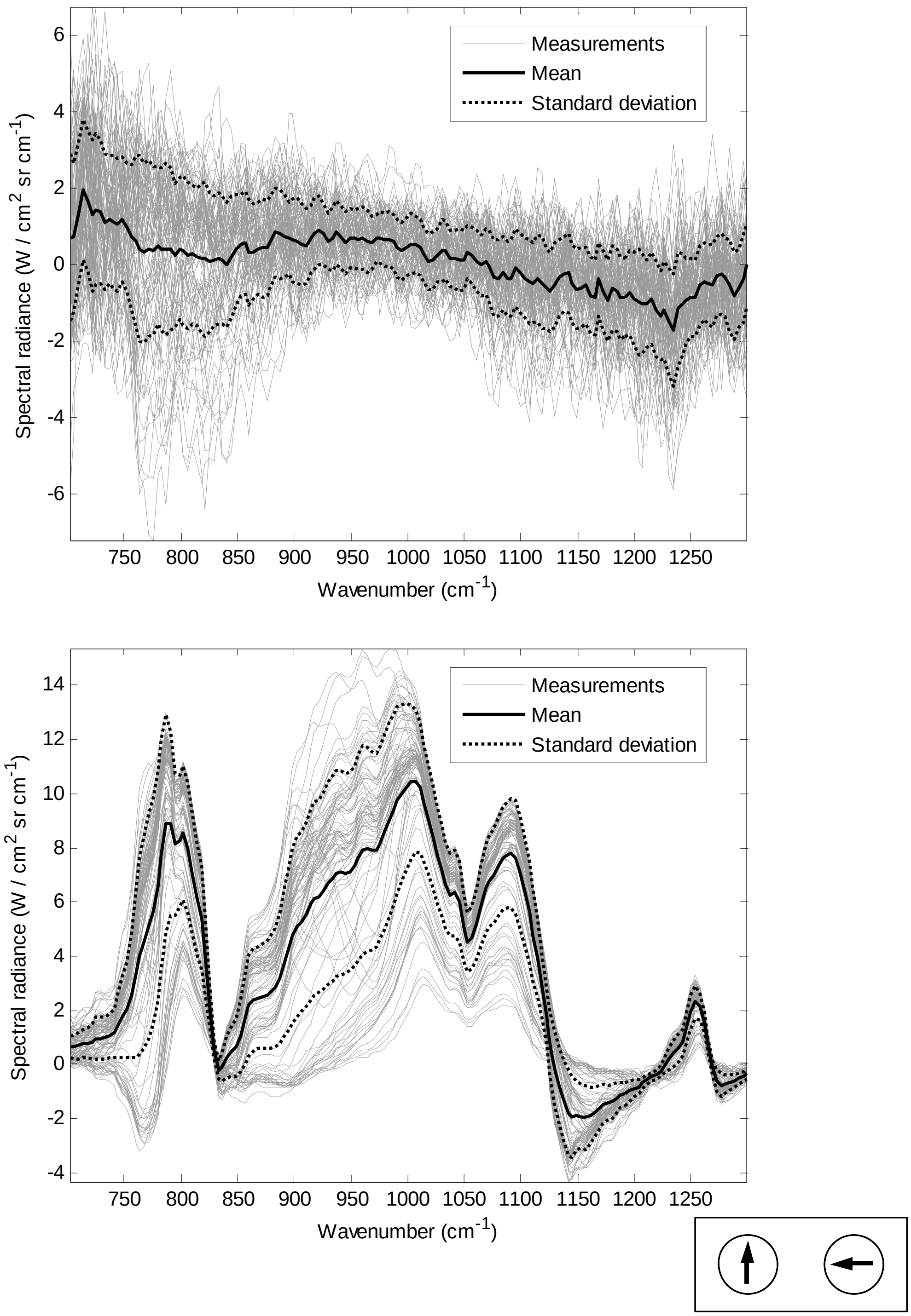

Figure 11. *Cross-polarised measurement of SF96 on water. Reference spectra of water (top graph) and spectra with 50 ml contamination (lower graph). The radiance values of the upper and lower graphs should be multiplied by 1×10^{-8} and 1×10^{-7}, respectively.*

5.2 Polarisation measurements of clouds

Polarised measurements were performed on cumulus clouds on October 19, 2004 at DRDC Valcartier. The calibration and reference spectra were made on a region with clear sky and the sensor was subsequently targeted at the clouds in order to obtain polarisation cloud measurements.

Figure 12 shows data collected with both polarisers aligned vertically with the background port closed (configuration (d) in Figure 3). The upper graph of Figure 12 shows the collected data when the target telescope was directed towards the clear sky region. The water bands are clearly distinguishable and the radiometric stability of the system and the environment is demonstrated. The lower graph of Figure 12 shows the measurements performed on the cumulus cloud where the water bands at 800-850 and 1200-1250 cm^{-1} and the ozone band at 975-1075 cm^{-1} can be clearly identified. The results obtained with this configuration are similar to the corresponding measurements obtained without polarisers, but with an inverted intensity [4]. The reason for this inversion is not currently understood.

Figure 13 describes the measurements taken with both polarisers aligned vertically (configuration (a) in Figure 3). The upper graph shows the data collection when the target and the background telescope were directed to the same clear sky region. The water and ozone bands are nonexistent due to the intrinsic capability of the dual-beam interferometer (CATSI) to optically subtract both input ports (target and background port). The lower graph of Figure 13 shows the measurements performed on a cloud after a calibration on a clear sky region. As expected, non-polarised spectra are collected and have the same characteristics as shown in previous data [4]. Water and ozone bands are clearly identified.

Figure 14 shows cross-polarisation measurements performed with the polariser in the target port aligned horizontally (configuration (f) in Figure 3). The upper graph of Figure 14 shows the reference spectra with both input ports directed to a clear sky region. The measurements indicate the radiometric stability of the instrument and the environment; however, the band that appears around 750-800 cm^{-1} is not identified. The lower graph of Figure 14 shows the collected data with cumulus cloud in the field of view. The spectra show characteristics bands of water (800-850 and 1200-1250 cm^{-1}) without ozone contribution. The radiance intensity seems to show an inversion around 1000 cm^{-1} when compared with the spectra in Figure 12.

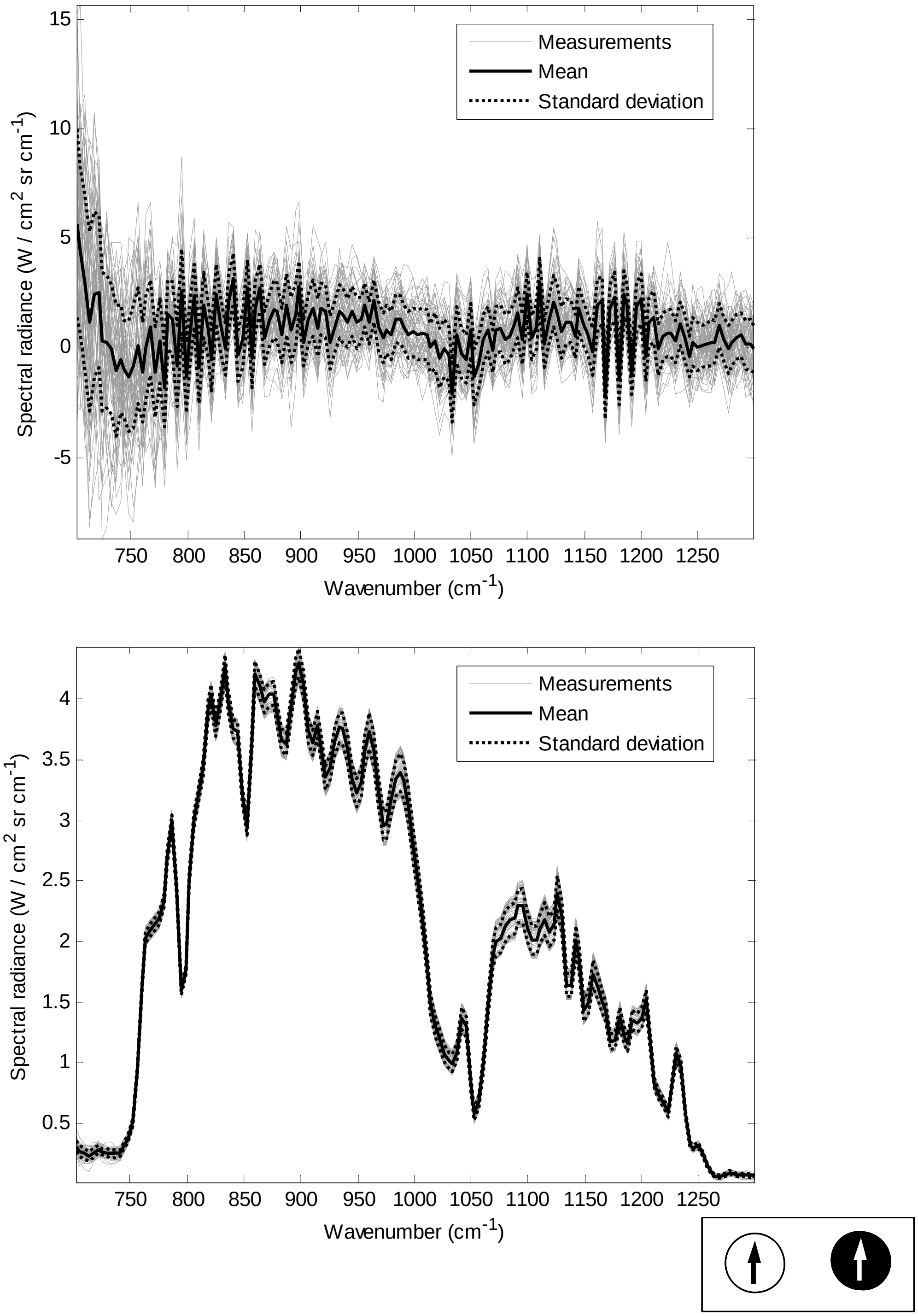

Figure 12. *Parallel-polarised measurement of cloud with background port closed. Reference spectra of clear sky (top graph) and spectra of cloud in the FOV (lower graph). The radiance values of the upper and lower graphs should be multiplied by 1×10^{-8} and 1×10^{-6}, respectively.*

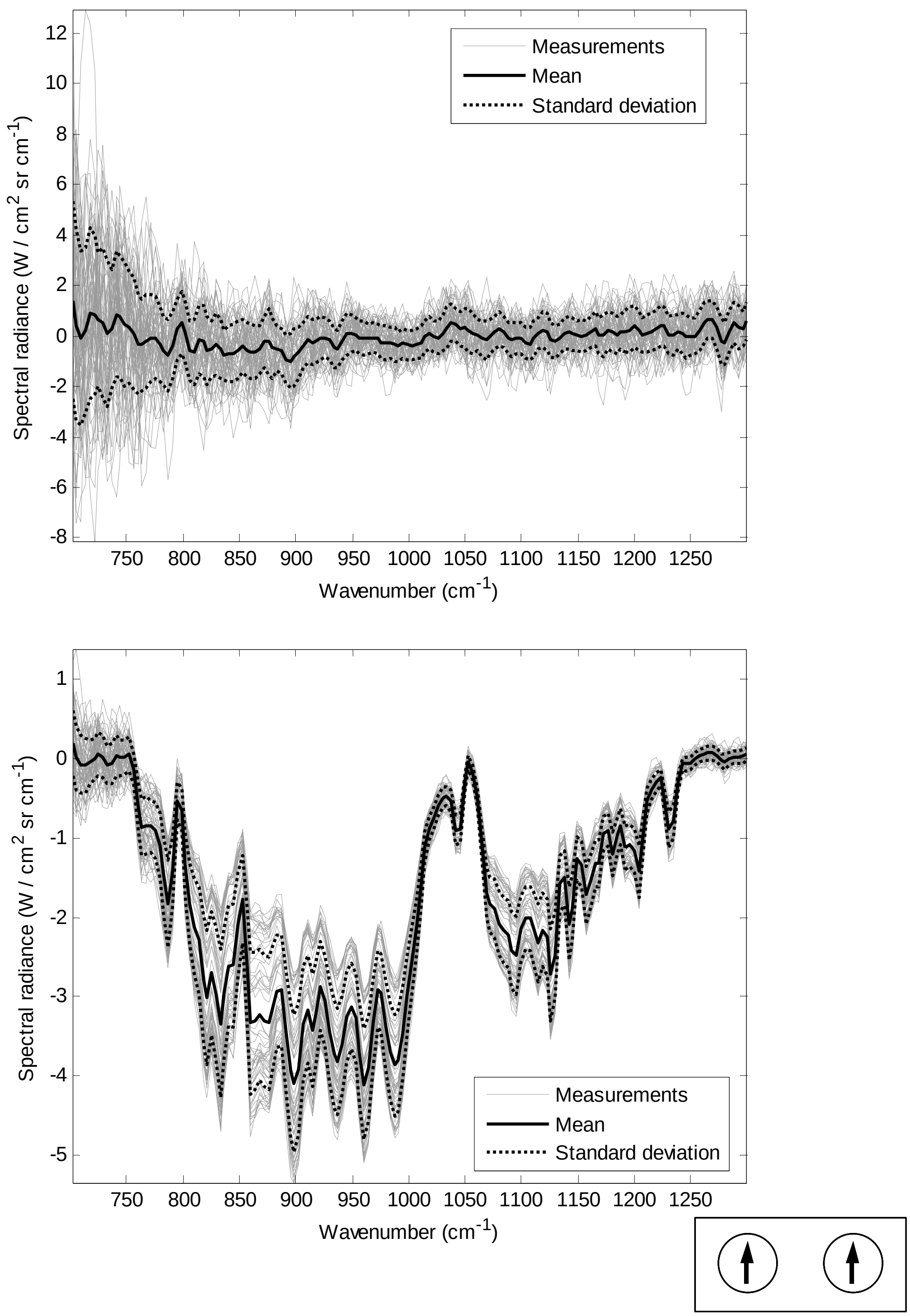

Figure 13. *Parallel-polarised measurement of cloud. Reference spectra of clear sky (top graph) and spectra of cloud in the FOV (lower graph). The radiance values of the upper and lower graphs should be multiplied by 1×10^{-8} and 1×10^{-7}, respectively.*

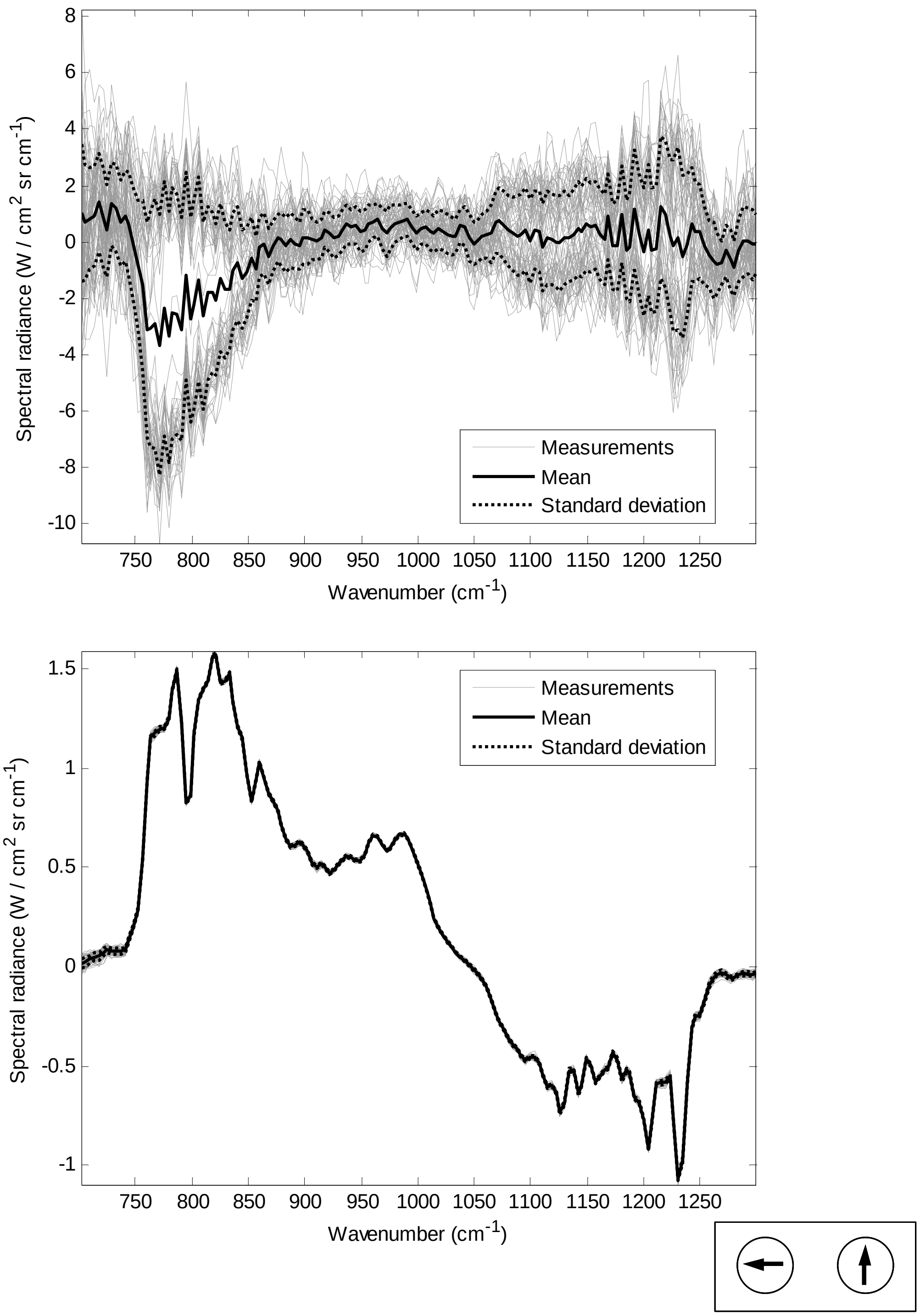

Figure 14. *Cross-polarised measurement of cloud. Reference spectra of clear sky (top graph) and spectra of cloud in the FOV (lower graph). The radiance values of the upper and lower graphs should be multiplied by 1×10^{-8} and 1×10^{-6}, respectively.*

6. Conclusion and future work

The novel approach of incorporating polarisers in the CATSI sensor system to measure differential polarised spectra was briefly investigated in order to evaluate the potential of this method for the detection of liquid contaminants on water surfaces. This approach seems to be promising but many phenomenological effects of surface and cloud polarisation need to be further investigated.

The angle of incidence used for these measurements will need to be validated to show if it can be optimized. The optimal angle of incidence may be different for each surface measured.

Simulations of the contaminant layer on water should be performed to reach a complete understanding of the contaminant-water system. Such simulations will require knowledge of the refractive index for all referential axes (x,y,z) for all studied contaminants. Complete understanding of the system will be achieved by modeling the polarimetric emission components.

The measurements on cumulus clouds show unexpected results and further simulations will be needed to fully understand the resulting data. However, the results appear to be promising and more data collection and analyses will be needed to understand the phenomenological atmospheric polarisation effects.

The results obtained during this measurement campaign show the potential of polarimetric dual-beam Fourier transform spectroscopy for measuring cross-polarised differential spectra; however, more work is needed to understand polarimetric phenomenological effects on the optics of the CATSI sensor.

The proposed spectral polarisation sensing approach and related phenomenology modeling is intended to significantly improve the signal-to-clutter ratio in the infrared remote sensing of surface contamination and hard target signatures.

7. References

1. J.-M. Thériault, “Passive Standoff Detection of Chemical Vapors by Differential FTIR Radiometry”, DREV TR 2000-156, January 2001, UNCLASSIFIED.

2. J.-M. Thériault, “Modeling the Responsivity and Self-emission of a Double-beam Fourier-transform infrared interferometer”, Appl. Opt., Vol. 38, 505-515, 1999.

3. J.-M. Thériault, E. Puckrin, D. Dubé, C. Bradette, J. Hancock, C. Chenier, P. Lecavalier, C.J. Lepage, S. Cairns, J.O. Jensen, F. D’Amico, C. Gittins and W. Marinelli “Passive Standoff Detection of Chemical Warfare Agent Contaminants on Surfaces : Laboratory and Field Trial Results for Liquid HD and VX”, DRDC Valcartier TR 2003-193, November 2003, UNCLASSIFIED.

4. J.-M. Thériault, “Remote Determination of Cloud Temperature and Transmittance from Spectral Radiance Measurements: Method and Results”, DREV R-9608, October 1996, UNCLASSIFIED.

List of symbols/abbreviations/acronyms/initialisms

BS	Beam Splitter
CATSI	Compact ATmospheric Sounding Interferometer
CC	Corner Cube
DRIFTS	Diffuse Reflectance Infrared Fourier-Transform Spectroscopy
FTIR	Fourier Transform InfraRed
FOV	Field of View
IRRAS	InfraRed Reflection Absorption Spectroscopy
PM-IRRAS	Polarisation Modulation - InfraRed Reflection Absorption Spectroscopy

Distribution list

INTERNAL

DRDC Valcartier ECR 2004-372

1 – Director General

3 – Document Library

1 – H. Lavoie (author)

1 – J.-M. Thériault (author)

1 – E. Puckrin (author)

1 – D. Dubé (author)

EXTERNAL

1 – DRDKIM (PDF file)
1 – Dr. James O. Jensen
U.S. Army SBCCOM
ATTN: SCBRD-RTE
Building E3549, Room C236
Aberdeen Proving Ground, MD 21010-5423
U.S.A.

DOCUMENT CONTROL DATA

1. ORIGINATOR (name and address) Defence R&D Canada Valcartier 2459 Pie-XI Blvd. North Québec, QC G3J 1X8	2. SECURITY CLASSIFICATION (Including special warning terms if applicable) Unclassified

3. TITLE (Its classification should be indicated by the appropriate abbreviation (S, C, R or U)

Polarisation measurement with a dual beam interferometer (CATSI) - Exploratory results and preliminary phenomenological analysis (U)

4. AUTHORS (Last name, first name, middle initial. If military, show rank, e.g. Doe, Maj. John E.)

Lavoie, H., Thériault, J.-M., Puckrin, E., Dubé, D.

5. DATE OF PUBLICATION (month and year) June 2006	6a. NO. OF PAGES 28	6b .NO. OF REFERENCES 4

7. DESCRIPTIVE NOTES (the category of the document, e.g. technical report, technical note or memorandum. Give the inclusive dates when a specific reporting period is covered.)

External Client Report

8. SPONSORING ACTIVITY (name and address)

9a. PROJECT OR GRANT NO. (Please specify whether project or grant) SDA-3090	9b. CONTRACT NO.
10a. ORIGINATOR'S DOCUMENT NUMBER ECR 2004-372	10b. OTHER DOCUMENT NOS N/A

11. DOCUMENT AVAILABILITY (any limitations on further dissemination of the document, other than those imposed by security classification)

- ☒ Unlimited distribution
- ☐ Restricted to contractors in approved countries (specify)
- ☐ Restricted to Canadian contractors (with need-to-know)
- ☐ Restricted to Government (with need-to-know)
- ☐ Restricted to Defense departments
- ☐ Others

12. DOCUMENT ANNOUNCEMENT (any limitation to the bibliographic announcement of this document. This will normally correspond to the Document Availability (11). However, where further distribution (beyond the audience specified in 11) is possible, a wider announcement audience may be selected.)

13. ABSTRACT (a brief and factual summary of the document. It may also appear elsewhere in the body of the document itself. It is highly desirable that the abstract of classified documents be unclassified. Each paragraph of the abstract shall begin with an indication of the security classification of the information in the paragraph (unless the document itself is unclassified) represented as (S), (C), (R), or (U). It is not necessary to include here abstracts in both official languages unless the text is bilingual).

This report presents preliminary results on the polarised long-wave infrared passive standoff detection and identification of surface contaminants and cumulus clouds using different polarisation configurations. The capability of the Compact ATmospheric Sounding interferometer (CATSI) for detecting chemical warfare (CW) surface contaminants is demonstrated from measurements of the CW simulant SF96 on water. Some polarimetric measurements of cumulus clouds were also performed to demonstrate the capability of polarisation measurements. The results obtained with the polarimetric dual-beam interferometer indicate that the signal-to-clutter ratio may be significantly improved in the infrared remote sensing of surface contamination and hard target signatures.

14. KEYWORDS, DESCRIPTORS or IDENTIFIERS (technically meaningful terms or short phrases that characterize a document and could be helpful in cataloguing the document. They should be selected so that no security classification is required. Identifiers, such as equipment model designation, trade name, military project code name, geographic location may also be included. If possible keywords should be selected from a published thesaurus, e.g. Thesaurus of Engineering and Scientific Terms (TEST) and that thesaurus-identified. If it is not possible to select indexing terms which are Unclassified, the classification of each should be indicated as with the title.)

CATSI, FTIR, LWIR, Polarisation, Surface contaminant, Water

Defence R&D Canada

Canada's Leader in Defence
and National Security
Science and Technology

R & D pour la défense Canada

Chef de file au Canada en matière
de science et de technologie pour
la défense et la sécurité nationale

DEFENCE R&D DÉFENSE

WWW.drdc-rddc.gc.ca